Final Draft
of the original manuscript:

Scheider, I.; Pfuff, M.; Dietzel, W.:
Simulation of hydrogen assisted stress corrosion cracking using the cohesive model
In: Engineering Fracture Mechanics (2007) Elsevier

DOI: 10.1016/j.engfracmech.2007.10.002

SIMULATION OF HYDROGEN ASSISTED STRESS CORROSION CRACKING USING THE COHESIVE MODEL

I. Scheider, M. Pfuff, W. Dietzel
GKSS Research Centre Geesthacht, Max-Planck-Str. 1, D – 21502 Geesthacht
Member of the Helmholtz Association of German Research Centres
ingo.scheider@gkss.de

ABSTRACT

This paper investigates the effect of hydrogen diffusion on stable crack propagation by using numerical finite element simulations based on the cohesive model. The model with its two common parameters, cohesive strength, T_0, and critical separation, δ_0, and its two additional parameters for stress corrosion cracking, the effective diffusivity, D_{eff}, and a material parameter, α, which represents the reduction of the cohesive strength, is described. This model is then employed to predict the stable crack propagation in C(T) specimens made from a high strength structural steel which were tested under hydrogen charging conditions in rising displacement tests using various deformation rates. It is shown that, in general, the prediction of stable crack propagation is promising, but may be further improved by the use of a more sophisticated diffusion equation. Finally, the influence of variations of the effective diffusivity and the cohesive strength reduction on the thus simulated crack growth resistance curves is studied.

Keywords hydrogen embrittlement; stress corrosion cracking; crack propagation; cohesive model; finite elements

Nomenclature

C	Hydrogen concentration	Γ	cohesive energy
D_{eff}	effective diffusivity	α	cohesive strength reduction factor
E'	Elastic modulus vor plane strain	δ_{BS}^{M}	CTOD acc. to British Standard
K	stress intensity factor	δ_5	CTOD, definition acc. to [15]
$\mathbf{T}$	cohesive traction vector	$\boldsymbol{\delta}$	material separation vector
T_0	cohesive strength	δ_1, δ_2	shape parameter for the traction-separation law
T^N	normal component of the cohesive traction	δ_0	critical separation
a_0	initial crack length	μ	normalized cohesive strength reduction factor
Δa	crack extension		

Introduction

Stress corrosion cracking (SCC) or, more general, environmentally assisted cracking, has long been recognised as a major cause for failure of engineering components and structures. The occurrence of SCC in a structure results from the combined action of sustained mechanical loading and a chemically aggressive environment. It often occurs without any visible deformation of the material and is difficult, if not impossible, to detect at early stages. One of the mechanisms leading to this environment induced failure is the embrittlement of the material due to the uptake of atomic hydrogen from the environment. Numerous models exist that describe material degradation and its effect on structural integrity caused by hydrogen embrittlement (HE). The proposed mechanisms on which these models are based include hydrogen enhanced decohesion (HEDE), hydrogen enhanced localized plasticity (HELP), adsorption induced dislocation emission (AIDE) and delayed hydride cracking (DHC). These mechanisms have been summarised by Lynch [1]. A useful basis for dealing with SCC and HE is offered by the fracture mechanics methodology. Using this methodology, fracture processes may be approached both theoretically and practically, providing an excellent framework for taking into account environmental effects on the failure phenomenon [2]. This framework is also extremely suitable for establishing parametric trends besides enabling the assessment of safety margins.

Most of these fracture mechanics approaches to SCC and HE are based on linear elastic fracture mechanics concepts, whereas more recent work often employs elastic-plastic fracture mechanics methodologies, i.e., the J integral and the crack tip opening angle/crack tip opening displacement, CTOA/CTOD. Models proposed by Vehoff et al. [3] and by Dietzel and Pfuff [4] involve the crack tip opening displacement, CTOD. In the present paper this approach is combined with a cohesive model approach.

Cohesive models which are based on considerations concerning the avoidance of the stress singularity at the crack tip introduced by Dugdale [5] and Barenblatt [6], have been used for the numerical simulation of ductile tearing of metals together with the finite element method since 1987 [7]. Nowadays, the numerical implementation using finite element techniques is such that interface elements are introduced which model the material separation, whereas the surrounding continuum elements are damage-free. These interface elements transfer cohesive stresses until they fail and form a crack.

The constitutive law of the cohesive model, the so-called traction-separation law, defines the dependence of the vector of cohesive tractions, $\mathbf{T} = \left(T^N, T^S, T^T\right)$, on the material separations in each direction, **δ**. For pure mode I fracture, a simple one-dimensional form $T^N = f(\delta^N)$ with two parameters, the cohesive strength, T_0, and the critical separation, δ_0, is sufficient to describe the material separation. The integral of the function $T(\delta)$ yields the total energy dissipated by the cohesive element, the cohesive energy, Γ_0.

During the last decade, the traction-separation law has been extended to include time-dependent processes, such as viscous (e.g., [8]) or rate dependent processes [9]. In the case of stress corrosion cracking, time dependence is related to the hydrogen diffusion into the material, which reduces the fracture toughness. Implementations of the diffusion process, which account for the effects of hydrostatic stresses and trapping by plastic deformation, have recently been introduced into cohesive modelling in models proposed by Serebrinsky et al. (SCO) [10] and by Liang and Sofronis (LS) [11]. The approach taken in these investigations makes use of the thermodynamically based finding that the hydrogen at the sites of the interface reduces the cohesive energy.

In the present paper, the diffusion process is described by the diffusion equation in its simplest form:

$$\frac{\partial C}{\partial t} = D_{\text{eff}} \nabla^2 C \quad , \tag{1}$$

where C is the bulk hydrogen concentration, and D_{eff} represents an effective diffusivity. In neglecting the hydrostatic stress term in the diffusion equation we assume that the initiation of failure takes place very close to the crack tip, and not in the region of high hydrostatic stress which is located in a distance corresponding to about two crack openings ahead of the crack tip. This assumption appears justified by the high concentration of hydrogen trapping sites near the crack tip, so that the total hydrogen concentration made up by hydrogen in lattice sites and hydrogen in traps is highest at the crack tip and decreases with the distance from the tip [12]. The peak of the hydrostatic stress modifies the distribution of lattice hydrogen, but it has an only week impact on the total hydrogen concentration in the region directly ahead of the crack tip. The effect of trapping on the hydrogen transport is accounted for by introducing an effective diffusion constant, D_{eff}.

The present paper addresses the validation of a concentration dependent cohesive model on the basis of experiments performed on a structural steel.

Numerical Model

The authors recently implemented interface elements for stable crack extension in ductile metals as user defined elements in the commercial finite element package ABAQUS® [13]. These elements are available for 2D and 3D models (see **Fehler! Verweisquelle konnte nicht gefunden werden.**) and represent the damage behaviour of the structure, while the surrounding continuum elements are damage free. The traction-separation law used for mode I failure condition is given by the following equation:

$$T = T_0\, f(\delta) = T_0 \begin{cases} 2\left(\dfrac{\delta}{\delta_1}\right) - \left(\dfrac{\delta}{\delta_1}\right)^2 & \delta < \delta_1 \\ 1 & \delta_1 < \delta < \delta_2 \\ 2\left(\dfrac{\delta - \delta_2}{\delta_0 - \delta_2}\right)^3 - 3\left(\dfrac{\delta - \delta_2}{\delta_0 - \delta_2}\right)^2 + 1 & \delta_2 < \delta < \delta_0 \end{cases} \tag{2}$$

Equation (2) contains two additional shape parameters, δ_1 and δ_2, which could be used to vary the shape of the traction-separation law, but are fixed as $\delta_1 = 0.05\,\delta_0$ and $\delta_2 = 0.65\,\delta_0$. The shape of the function is shown in **Fehler! Verweisquelle konnte nicht gefunden werden.** (right).

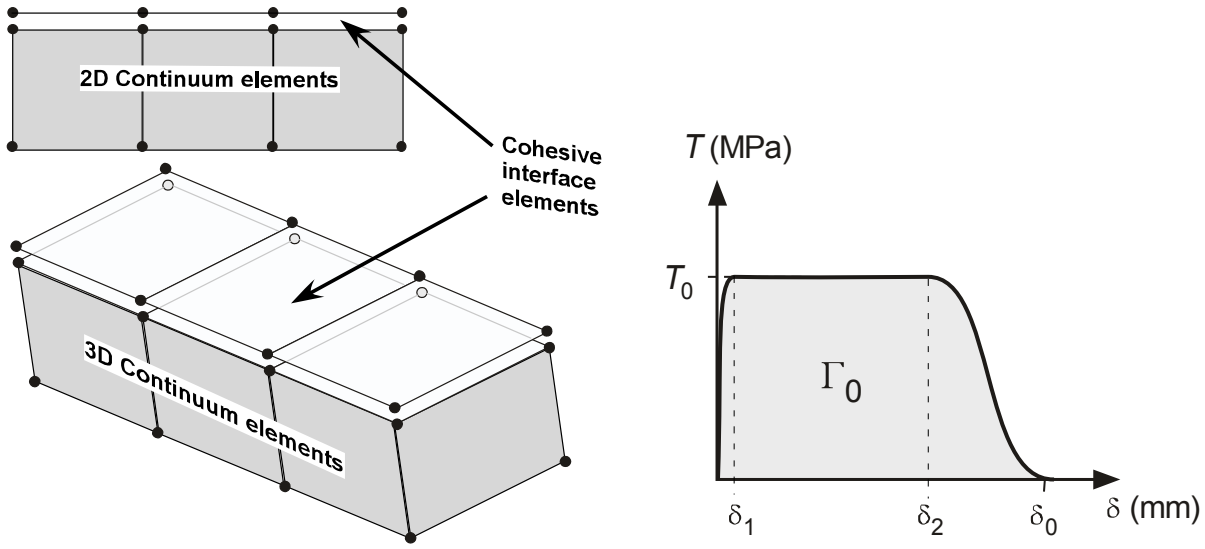

Figure 1: Sketch of cohesive interfaces and continuum elements (left); traction-separation law given by Eq. (2) (right).

The existing implementation was now extended to cover the degradation of the damage properties due to the hydrogen diffusion process. As in [10, 11] it is assumed that the cohesive strength, T_0, is reduced by hydrogen, whereas the critical separation, δ_0, remains constant. For low values of the hydrogen concentration the cohesive parameter T_0 is assumed to linearly depend on the hydrogen concentration, C,

$$T_{0,Hyd} = T_0(1 - \alpha C)\,, \tag{3}$$

where α is an unknown material parameter with the dimension [1/concentration].

It should be noted that the approach taken here is similar to the one proposed in [14], according to which the failure strain, ε_f, decreases linearly with the local hydrogen concentration. It assumes that the concentration is sufficiently low to suppress non-linear effects like those addressed in the SCO model [10].

The spatial hydrogen concentration gradient, eq. (1), is considered in crack propagation direction only and is only evaluated in the cohesive elements. The boundary condition for the hydrogen is such that a fixed environmental concentration, C_{env}, is assumed at the moving crack tip. This means that, once a cohesive element has failed, it takes the value of C_{env}. As initial condition it is assumed that the hydrogen concentration of the cohesive elements is zero, whereas the concentration C_{env} is available at the crack flanks.

The cohesive energy dissipated by the cohesive element,

$$\Gamma_{0,hyd} = \int_0^{\delta_0} T(\delta)\mathrm{d}\delta = T_0 \int_0^{\delta_0} (1-\alpha C)\, f(\delta)\,\mathrm{d}\delta\,. \tag{4}$$

is reduced at most by the factor (1-αC_{env}), if and only if the hydrogen concentration is equal to the environmental one.

A parameter $\mu = \alpha\, C_{\mathrm{env}}$ is introduced, which depends on both the material and the environmental conditions, can take values between 0 and 1 and controls the effect of hydrogen on the cohesive strength. Since C_{env} cannot directly be measured, μ has to be determined by comparing the simulated R-curves with the measured ones.

Experimental Validation

The concentration dependent cohesive model was validated by experiments performed on a high strength, low alloy structural steel with the German designation FeE 690T. The mechanical properties of the material, which in strength and composition may to some extent be compared with the pipeline steel X100, are $R_{\mathrm{p0.2}}$ = 695 MPa and R_{m} = 820 MPa [4]. It is assumed that yield strength and hardening do not vary with hydrogen concentration. The failure strain reduction, however, is captured by the reduction of cohesive strength. The experimental true stress – logarithmic strain curve and the curve that is used for the numerical simulations are shown in Fehler! Verweisquelle konnte nicht gefunden werden..

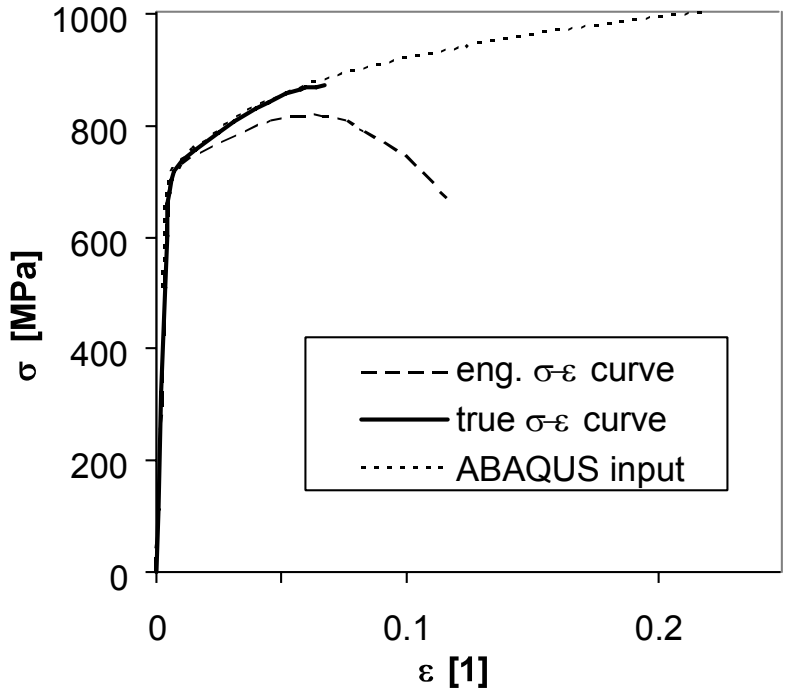

Figure 2: Stress-strain curve of the material under consideration, FeE690T, from [4].

A series of pre-cracked C(T) specimens with a width $W = 40$ mm, thickness $t = 19$ mm and an initial crack length to width ratio of $a_0/W \approx 0.55$ were tested in laboratory air and in ASTM substitute ocean water under hydrogen charging conditions [4]: A cathodic potential of -900 mV vs. Ag/AgCl electrode was applied to the specimens during the tests in order to promote this hydrogen charging. From these experiments performed at various load-line displacement rates, CTOD R-curves, measured in terms of δ_{BS}^{M} [15] vs. Δa, were generated. In principle, the crack tip opening displacement can directly be measured at laboratory specimens as well as on real components whose structural behaviour is to be assessed. In the form of the so-called "δ_5" it is obtained as the displacement of two points located 2.5 mm above and below the tip of the starter crack. In SCC experiments, however, which usually are performed in corrosive environments, particularly in aqueous chloride solutions and/or at elevated temperatures, a direct measurement of δ_5 is tedious since the gauge for measuring has to be immersed in the corrosion environment for the duration of the test and hence has to be carefully protected. However, as has been shown in previous work, an excellent agreement exists between measured δ_5 values and values which are inferred from the load and load line displacement using a modified version of the British Standard 5762 allowing for crack growth [16, 17, 18]:

$$\delta_5 = \delta_{BS}^{M} = \frac{K^2}{2\sigma_y E'} + \frac{0.6\Delta a + 0.4(W - a_0)}{0.6(a_0 + \Delta a) - 0.4W + z} \cdot v_{pl} \tag{5}$$

In this modified BS CTOD, δ_{BS}^{M}, the motion of the specimen's rotation centre due to the crack growth is taken into account. The variable v_{pl} is the plastic portion of the crack mouth opening displacement (*CMOD*), z is the distance between the load line

and the actual measuring position for v, and E' is the Young's modulus for plane strain. The CTOD R-curves thus obtained are shown in **Fehler! Verweisquelle konnte nicht gefunden werden.** and in the following compared with the numerical results.

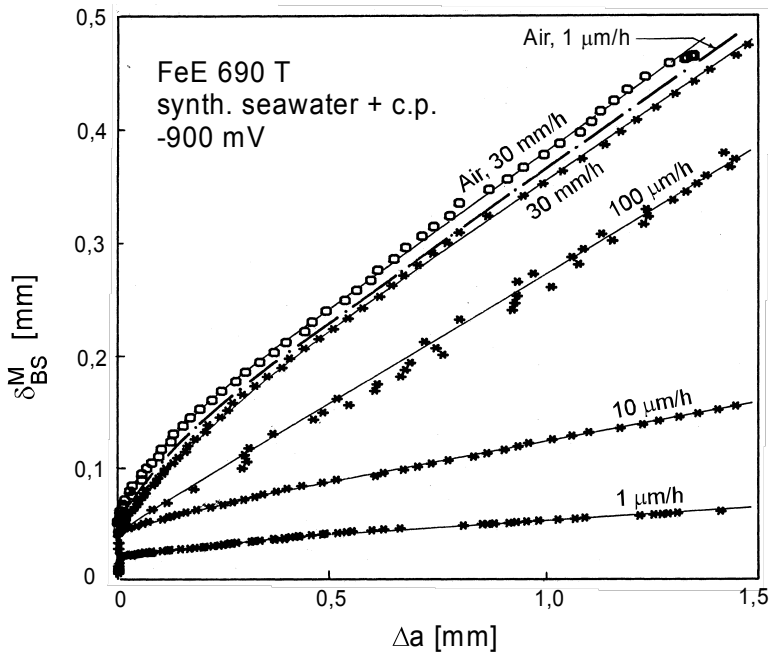

Figure 3: Experimental CTOD R-curves obtained from C(T) specimens tested in air and under hydrogen charging conditions at various constant load-line displacement rates, indicated at the curves [16].

In a first step, the cohesive parameters - without any influence of hydrogen - were determined. A 2D plane strain model of the C(T) specimen was generated with a cohesive line along the ligament. Due to symmetry conditions, only one half of the structure was modelled. For the deformation behaviour of the structure, von Mises plasticity with pure isotropic hardening (dotted curve in **Fehler! Verweisquelle konnte nicht gefunden werden.**) was used. The fracture test under lab air conditions was reproduced by a cohesive model simulation with varying parameters T_0 and δ_0 in order to derive their optimal values. This study yielded T_0 = 2440 MPa and δ_0 = 0.016 mm, resulting in a separation energy of Γ_0 = 32 kJ/m². These parameters were used in all subsequent calculations. A comparison between the numerical and the experimental R-curves is shown in **Fehler! Verweisquelle konnte nicht gefunden werden.**.

The additional parameters taking the effect of hydrogen diffusion into account, i.e., the effective diffusivity, D_{eff}, and the strength reduction factor, μ, were adopted from a systematic variation of these parameters in the numerical simulation for a load-line displacement rate of 0.01 mm/h. The curve fitting yields $D_{eff} = 2 \cdot 10^{-6}$ mm²/s and $\mu = 0.2$. Here, the value of D_{eff} is in good agreement with experimental data which had been determined in a previous investigation by Dietzel et al. [19]. In this earlier work, for the same material the influence of the local plastic strain on the effective

diffusion coefficient had been studied yielding a value of D_{eff} in the range of$\cdot 8 \cdot 10^{-7}$ to $2 \cdot 10^{-6}$ mm²/s in the vicinity of a crack tip in a C(T) specimen.

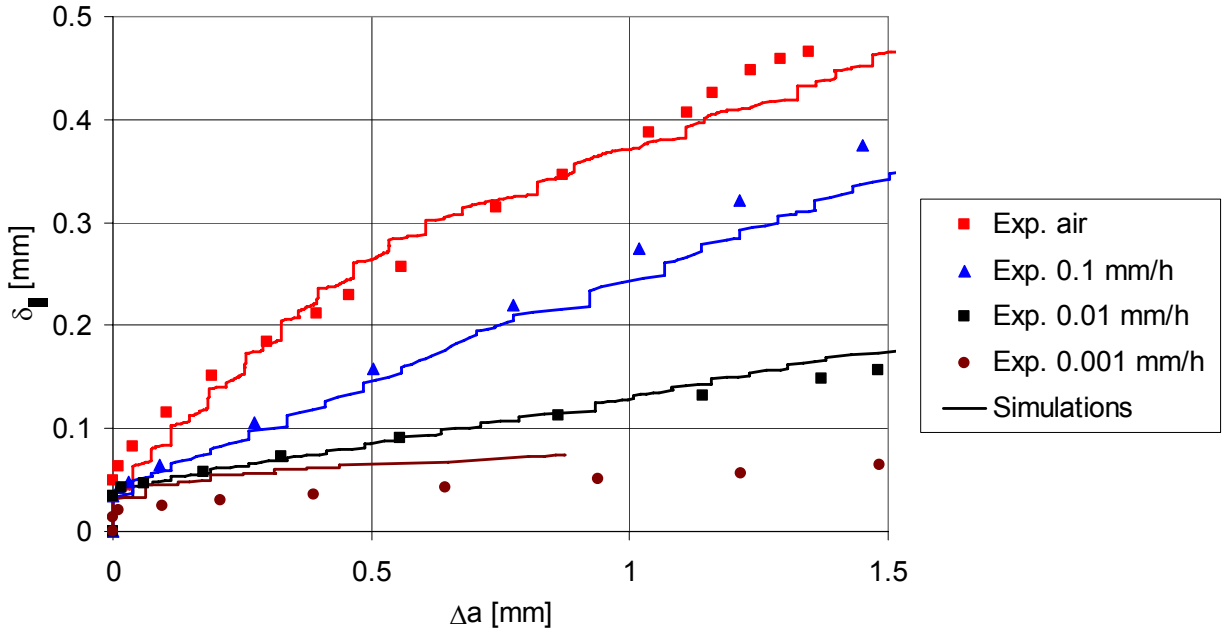

Figure 4: Comparison of experimental and simulated CTOD R-curves for hydrogen charging conditions (displacement rates: 0.1, 0.01 and 0.001 mm/h) and in laboratory air.

The calculated R-curve thus fitted to the experimental curve for a load-line displacement rate of 0.01 mm/h is shown in **Fehler! Verweisquelle konnte nicht gefunden werden.** together with the simulated and experimental curves for the displacement rates 0.001 mm/h and 0.1 mm/h. The comparison shows that the degradation is predicted quite well for 0.1 mm/h. For the slowest rate, the reduction of the CTOD at crack initiation is underestimated, but the overall behaviour is still predicted fairly well. Convergence has not been reached after 1 mm crack extension for this simulation; this is probably due to an instability, i.e. the elastic energy stored in the specimen would lead to failure of several cohesive elements at a time.

It is worth noting that the reduction in cohesive strength, expressed by the factor μ, is rather low, and the cohesive energy is significantly reduced only at the onset of crack extension (from 32 kJ/m² down to 25.6 kJ/m²). The dissipated separation energy, $\Gamma_{0,\mathrm{hyd}}$, increases with the growing crack, especially for higher loading rates, as is indicated by the curves shown in Fehler! Verweisquelle konnte nicht gefunden werden.. The behaviour of the curves explains to a large extent the simulated CTOD R-curves, as shown in Fehler! Verweisquelle konnte nicht gefunden werden., especially, the small variation of CTOD for different displacement rates at crack initiation. The curves in Fehler! Verweisquelle konnte nicht gefunden werden. display the relative hydrogen concentration ahead of the crack tip at crack initiation and at Δa = 1, 2.5 and 4 mm, respectively (for the loading rate v = 0.001 mm/h the concentration is only available for Δa = 1 mm due to numerical difficulties). Obviously

the hydrogen distribution is reduced during the initial states of crack growth and, due to a constant crack growth rate, reaches a steady state distribution after a few millimetres.

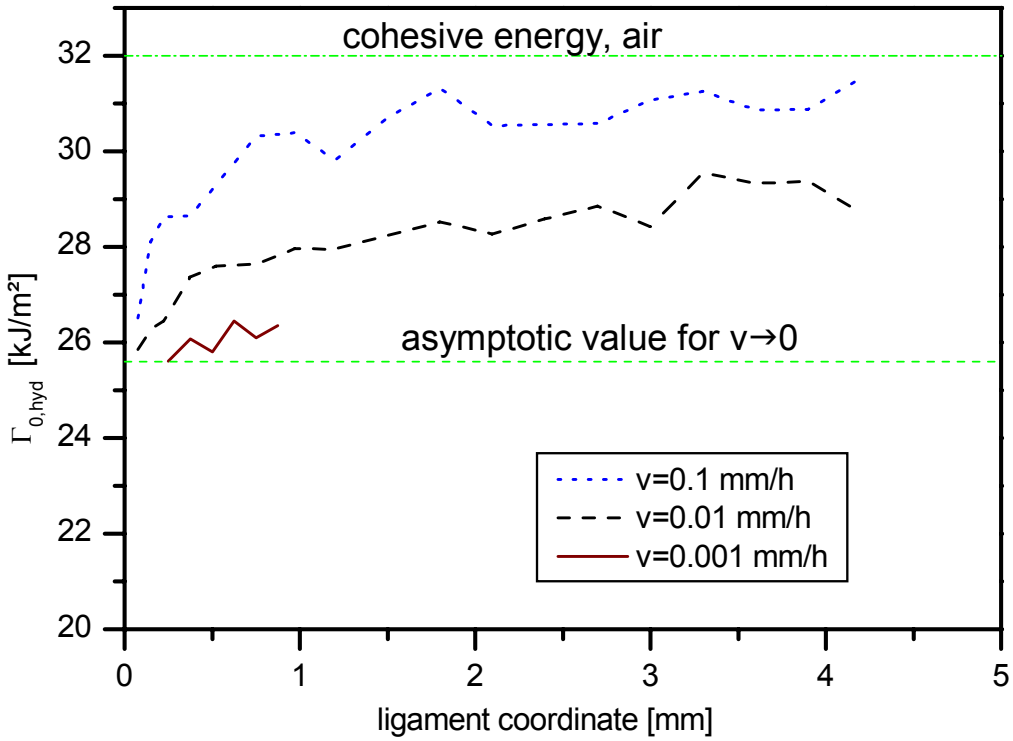

Figure 5: Separation energies of the ligament reduced by hydrogen charging.

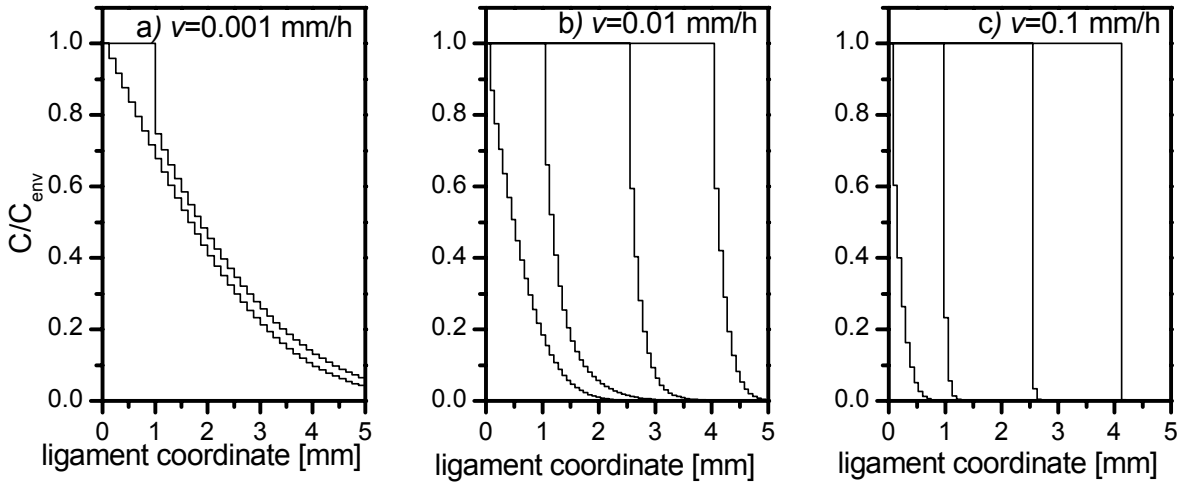

Figure 6: Relative hydrogen concentration in the ligament at crack initiation, Δa=1 mm, 2.5 mm, and 4 mm, respectively, for different loading rates: a) v = 0.001mm/h, b) v = 0.01mm/h, c) v = 0.1mm/h.

It is expected that a more sophisticated diffusion equation, e.g. the one proposed by Krom et al. [20], which takes the effect of plastic strain on the diffusivity into account, may improve the accuracy of the predictions.

Parameter Sensitivity

It was assessed, how a variation of the two parameters D_{eff} and μ affect the results of the simulations. To this end, the diffusivity was varied between $2 \cdot 10^{-5}$ and $2 \cdot 10^{-7}$ mm²/s, while μ was kept fixed at 0.2, and the cohesive strength reduction, μ, was varied between 0.1 and 0.9 with D_{eff} in turn being kept fixed.

The results of this sensitivity analysis are shown in **Fehler! Verweisquelle konnte nicht gefunden werden.**a for a variation of the diffusivity and in **Fehler! Verweisquelle konnte nicht gefunden werden.**b for the variation of the reduction factor. Since the simulation in air is equivalent to a vanishing diffusivity or a zero reduction factor, this simulation is included in both these figures. The effect of both parameters is comparable, but can be distinguished: While the diffusivity D_{eff} affects the slope of the complete R-curve, but has only minor influence on the crack initiation, the strength reduction factor μ mainly affects the first part of crack propagation, i.e., $\Delta a < 1$ mm. It can also be seen that a reduction factor of 0.5 or higher does not change the R-curve behaviour significantly. This is due to the fact that a reduction of the cohesive strength leads to a lower plasticity ahead of the crack tip. It should be noted that the dependence of the cohesive strength on the hydrogen concentration differs significantly from the dependence of the failure strain on the hydrogen concentration as proposed in [14] for the same material. In this latter study, due to the strain hardening behaviour of the material under investigation, a given reduction in strength would correspond to a much more pronounced reduction of the critical strain.

It is worth noting that due to the simple form of the differential equation (1) and the linearity of Eq. (3) in the hydrogen concentration, a change in effective diffusivity is equivalent to a change in deformation rate. Therefore, the curve for $D_{eff} = 2 \cdot 10^{-7}$ mm²/s and a load-line displacement rate of 0.01 mm/h in **Fehler! Verweisquelle konnte nicht gefunden werden.**a is the same as the one for 0.10 mm/h with the original parameters shown in **Fehler! Verweisquelle konnte nicht gefunden werden.**.

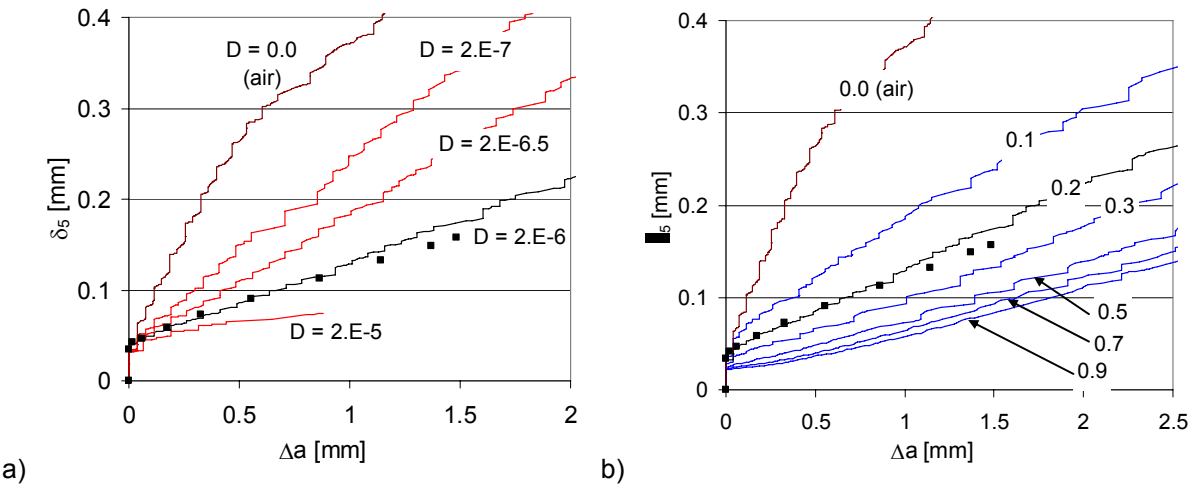

Figure 7: Sensitivity of the simulation on the cohesive parameters for stress corrosion cracking; a) the effective diffusivity, Deff given in mm²/s; b) the cohesive strength reduction factor, μ.

Conclusions

The cohesive model for numerical crack propagation simulations was extended to include the effect of hydrogen embrittlement on flawed specimens. The model was applied to a structural steel, which was tested at various load-line displacement rates in ASTM substitute ocean water using cathodic polarisation to promote hydrogen embrittlement. Two parameters which characterise the mechanical properties of the material and which are independent of the hydrogen uptake were determined by fitting the simulated crack propagation behaviour in air to the experimental results. Two additional parameters reflecting the hydrogen embrittlement, i.e., the effective diffusivity, D_{eff}, and the cohesive strength reduction factor, μ, were determined by fitting the result of the simulation for a specific displacement rate (0.01 mm/h) to the corresponding experimental data obtained under hydrogen charging. Based on this, R-curves for two other displacement rates were predicted without any further adjustment of the parameters. It was shown that even though the diffusion equation, Eq. (1), in its simplest form does not explicitly account for the influence of the plastic deformation on the diffusivity, the predictions were quite successful. However, the parameter identification resulted in a small cohesive strength reduction ($\mu = 0.2$). Since the critical separation was kept constant, the reduction of the crack tip opening displacement at initiation, which was significant for very low loading rates, could not be reproduced by the simulations. It is suspected that the assumption of a constant critical separation, which has been adopted from other authors [10, 11], is too strict. In addition, it is expected that a more appropriate characterisation of the hydrogen diffusion would improve the accuracy of the crack propagation behaviour predicted. This could be, for example, the differential equation proposed in [20] which distinguishes between lattice and trap concentration of hydrogen and which assumes a stress dependence of the lattice concentration.

A sensitivity analysis with respect to the parameters D_{eff} and μ reveals that these parameters influence the crack extension behaviour in a specific way: Because of the simple form of the diffusion equation used a change in the diffusivity has the same effect as a change in the displacement rate, both result in a change of the slope of the corresponding R-curve. On the other hand, a higher value of the reduction factor μ causes a reduction of the CTOD value at crack initiation and a slower rise in the beginning of the R-curve (up to Δa = 1 mm).

References

1. Lynch S.P., Mechanisms of Hydrogen Assisted Cracking - A Review. In: *Hydrogen Effects on Material Behaviour and Corrosion Deformation Interactions*, Eds. N.R. Moody, A.W. Thompson, R.E. Ricker, G.W. Was, R.H. Jones, TMS, 449-466, 2003.

2. Dietzel, W. and Turnbull, A., Comprehensive Structural Integrity, Vol. 11 Ch. 11.04, Stress Corrosion Cracking, K.-H. Schwalbe (Ed.), Elsevier Science Ltd., Amsterdam, 2006, in preparation (online edition).

3. Vehoff, H., Stenzel, H. and Neumann, P., Experiments on bicrystals concerning the influence of localized slip on the nucleation and growth of intergranular stress corrosion cracks. *Z. Metallkunde* **78**, 550-556, 1987.

4. Dietzel, W. and Pfuff, M., The effect of deformation rates on hydrogen embrittlement. In: *Hydrogen Effects in Materials*. Eds. A.W. Thompson and N.R. Moody, The Minerals and Materials Society, 303-311, 1996.

5. Dugdale, D. S., Yielding of steel sheets containing slits. *J. Mech. Phys. Solids* **8**, 100-104, 1960.

6. Barenblatt, G. I., The mathematical theory of equilibrium cracks in brittle fracture. *Adv. Appl. Mech.* **7**, 55-129, 1962.

7. Needleman, A., A continuum model for void nucleation by inclusion debonding. *J. Appl. Mech.* **54**, 525-531, 1987.

8. Corigliano, A. and Ricci, M., Rate-dependent interface models: formulation and numerical applications. *Int. J Solids Struct.* **38**, 547-576, 2001.

9. Costanzo, F. and Walton, J. R., A study of dynamic crack growth in elastic materials using a cohesive zone model. *Int. J. Eng. Sci.* **35**, 1085–1114, 1997.

10. Serebrinsky, S., Carter, E.A. and Ortiz, M., A quantum-mechanically informed continuum model of hydrogen embrittlement. *J. Mech. Phys. Solids* **52**, 2403-2430, 2004.

11. Liang, Y. and Sofronis, P., Toward a phenomenological description of hydrogen-induced decohesion at particle/matrix interfaces. *J. Mech. Phys. Solids* **51**, 1509-1531, 2003.

12. Sofronis, P. and McMeeking, R.M., Numerical analysis of hydrogen transport near a blunting crack tip. *J. Mech. Phys. Solids* **37**, 317-350, 1989.

13. Scheider, I., Simulation of cup-cone fracture in round bars using the cohesive zone model. In: *First M.I.T. Conf. on Comp. Fluid and Solid Mech.*, Ed. K.J. Bathe, Elsevier, Amsterdam, 460-462, 2001.

14. Pfuff, M. and Dietzel, W., Mesoscale modelling of hydrogen assisted crack growth in heterogeneous materials. In: *Proc. of the 11th Int. Conf. on Fracture*, Turin (Italy), Ed. A. Carpinteri, 2005.

15. Dietzel, W. and Daum, K.-H., δ_5 and SCC - A new approach to an old problem. In: *The life of a crack; Initiation – Growth – Fracture*. Ed: M. Kocak, Report GKSS Forschungszentrum Geesthacht, 2001.

16. Dietzel, W., Zur Anwendung bruchmechanischer Methoden bei der Untersuchung des Umgebungseinflusses auf die Rissausbreitung bei zügiger Beanspruchung, PhD Thesis, Technische Universität Hamburg-Harburg, 1990 (in German).

17. Hellmann, D. and Schwalbe, K.-H.; On the Experimental Determination of CTOD Based R-Curves. In: *The Crack Tip Opening Displacement in Elastic-Plastic Fracture Mechanics*, Ed. K.-H. Schwalbe, Springer Verlag, Berlin-Heidelberg-New York, 1986.

18. British Standard BS 5762; Methods of Tests for Crack Opening Displacement (COD) Testing, British Standards Institution (Gr. 6), London, 1979

19. Dietzel, W., Pfuff, M. and Juilfs, G., Investigations of hydrogen transport in plastically deformed steel membranes. In: *Proc. of 2nd Int. Conf. on Environmental Degradation of Engineering Materials*, EDEM 2003, Bordeaux (France), 2003.

20. Krom, A.H.M., Koers, R.W.J. and Bakker, A., Hydrogen transport near a blunting crack tip, *J. Mech. Phys. Solids* **47**, 971-992, 1999.